

On relations of anisotropy and linear inhomogeneity using Backus average

Md Abu Sayed*, Theodore Stanoev†

Abstract

The anisotropy of an equivalent medium resulting from the Backus (1962) average is induced by the vertical inhomogeneity among its constituent layers. The velocity field of the constituent isotropic layers increases linearly with depth, which is assumed to be a good seismological description of sedimentary layers (Slotnick, 1959). We derive an analytical relationship between the anisotropy, characterized by the Thomsen (1986) parameters, and the linear inhomogeneity parameters, which forms a system of three equations for nine unknowns. To obtain well-posedness, we constrain the problem by considering two seismological methods applied to field data. We use the results from the two methods, for a particular region of interest, to assess the validity of the analytical relation.

1 Introduction

In this article, we parameterize an equivalent medium, resulting from the Backus (1962) average, with respect to linear inhomogeneity parameters of its constituent isotropic layers. Sedimentary basins often show thin layers that induce seismic anisotropy. The parametrization allows us to make a relationship between the anisotropy to layer inhomogeneity, which is, in seismological context, an important relation. We also assume the medium possesses linear inhomogeneity, which was first introduced by Slotnick (1959). The traveltime expression from a source to a receiver in a linearly inhomogeneous media is shown by Slawinski and Slawinski (1999).

To obtain a solution from the analytical relationship between the anisotropy and the linear inhomogeneity parameters, we require to provide one of the inhomogeneity parameter. We use two independent seismological methods, 1-D tomography and *ab* model, to make the analytical relation to be well posed. The outcomes of the seismological methods are a pair of inhomogeneity parameters, using one of the parameter from each method allows us to obtain the solution of the analytical relation. The resultant solution from the analytical relation then can be examined by comparing with the results of the seismological methods.

2 Equivalent medium parameterization

We parameterize a transversely isotropic equivalent medium resulting from the Backus average of thin, intrinsically homogeneous, isotropic layers, which we refer to as the *Backus medium*. We assume that a stack of such constituent layers is inhomogeneous and possesses a constant-velocity gradient that increases linearly with depth (see e.g., Slawinski and Slawinski, 1999). Specifically, for both *P* and *S* waves,

$$v_P(z) = a_P + b_P z \quad \text{and} \quad v_S(z) = a_S + b_S z, \quad (1)$$

where $a_{P,S}$ are the wavespeeds at the top of the medium, $b_{P,S}$ are positive velocity-gradient constants, and z is the depth.

*Department of Earth Sciences, Memorial University of Newfoundland, m.abusayed.stu@gmail.com

†Department of Earth Sciences, Memorial University of Newfoundland, theodore.stanoev@gmail.com

2.1 Backus average

Following the definition of Backus (1962, Section 3), the average of a function $f(z)$ of width ℓ' is the moving average given by

$$\bar{f}(z) = \int_{-\infty}^{\infty} w(\zeta - z) f(\zeta) d\zeta, \quad (2)$$

where the properties of the weighting function are

$$w(z) \geq 0, \quad w(\pm\infty) = 0, \quad \int_{-\infty}^{\infty} w(z) dz = 1, \quad \int_{-\infty}^{\infty} z w(z) dz = 0, \quad \int_{-\infty}^{\infty} z^2 w(z) dz = (\ell')^2.$$

The result of performing average (2) on isotropic layers results is a homogeneous TI medium, where the corresponding elasticity parameters, which are referred to as *Backus parameters*, are

$$\bar{c}_{1111}^{\text{TI}} = \overline{\left(\frac{c_{1111} - 2c_{2323}}{c_{1111}}\right)^2} \overline{\left(\frac{1}{c_{1111}}\right)^{-1}} + \overline{\left(\frac{4(c_{1111} - c_{2323})c_{2323}}{c_{1111}}\right)}, \quad (3a)$$

$$\bar{c}_{1122}^{\text{TI}} = \overline{\left(\frac{c_{1111} - 2c_{2323}}{c_{1111}}\right)^2} \overline{\left(\frac{1}{c_{1111}}\right)^{-1}} + \overline{\left(\frac{2(c_{1111} - 2c_{2323})c_{2323}}{c_{1111}}\right)}, \quad (3b)$$

$$\bar{c}_{1133}^{\text{TI}} = \overline{\left(\frac{c_{1111} - 2c_{2323}}{c_{1111}}\right)} \overline{\left(\frac{1}{c_{1111}}\right)^{-1}}, \quad (3c)$$

$$\bar{c}_{1212}^{\text{TI}} = \overline{c_{2323}}, \quad (3d)$$

$$\bar{c}_{2323}^{\text{TI}} = \overline{\left(\frac{1}{c_{2323}}\right)^{-1}}, \quad (3e)$$

$$\bar{c}_{3333}^{\text{TI}} = \overline{\left(\frac{1}{c_{1111}}\right)^{-1}}. \quad (3f)$$

Since the weighting function, w , in integral (2), is continuous and symmetric, the Backus average may be written as a weighted average (e.g., Slawinski, 2018, Section 4.2.2). Herein, the Backus average is weighted by layer thickness. For density-scaled VSP measurements, $v_P = \sqrt{c_{1111}}$ and $v_S = \sqrt{c_{2323}}$; this allows for a reparameterization of parameters (3a)–(3f) in terms of linear-inhomogeneity parameters (1). For example, Backus parameter (3d) may be rewritten as

$$\begin{aligned} \bar{c}_{1212}^{\text{TI}} = \overline{c_{2323}} &= \frac{1}{h_2 - h_1} \int_{h_1}^{h_2} c_{2323} dz = \frac{1}{h_2 - h_1} \int_{h_1}^{h_2} (a_S + b_S z)^2 dz \\ &= \frac{1}{3} (3a_S^2 + 3a_S b_S (h_1 + h_2) + b_S^2 (h_1^2 + h_1 h_2 + h_2^2)). \end{aligned} \quad (4)$$

For Backus parameter (3a), we begin with the first term, where

$$\overline{\left(\frac{c_{1111} - 2c_{2323}}{c_{1111}}\right)} = \frac{1}{h_2 - h_1} \int_{h_1}^{h_2} \left(1 - 2\frac{v_S^2}{v_P^2}\right) dz = \frac{1}{h_2 - h_1} \int_{h_1}^{h_2} \left(1 - 2\frac{(a_S + b_S z)^2}{(a_P + b_P z)^2}\right) dz = 1 - \frac{2I_1}{h_2 - h_1} \quad (5)$$

and

$$\begin{aligned}
I_1 &= \int_{h_1}^{h_2} \frac{(a_S + b_S z)^2}{(a_P + b_P z)^2} dz = \frac{h_2 b_S^2}{b_P^2} - \frac{h_1 b_S^2}{b_P^2} \\
&+ \frac{\ln(a_P + h_1 b_P) (2 a_P b_S^2 - 2 a_S b_P b_S)}{b_P^3} - \frac{\ln(a_P + h_2 b_P) (2 a_P b_S^2 - 2 a_S b_P b_S)}{b_P^3} \\
&+ \frac{a_P^2 b_S^2 - 2 a_P a_S b_P b_S + a_S^2 b_P^2}{b_P (h_1 b_P^3 + a_P b_P^2)} - \frac{a_P^2 b_S^2 - 2 a_P a_S b_P b_S + a_S^2 b_P^2}{b_P (h_2 b_P^3 + a_P b_P^2)}. \quad (6)
\end{aligned}$$

For the second term in parameter (3a),

$$\left(\frac{1}{c_{1111}} \right)^{-1} = \left(\frac{1}{v_P^2} \right)^{-1} = \left(\frac{1}{h_2 - h_1} \int_{h_1}^{h_2} \frac{1}{(a_P + b_P z)^2} dz \right)^{-1} = (h_2 - h_1) \left(\int_{h_1}^{h_2} (a_P + b_P z)^{-2} dz \right)^{-1}.$$

Substituting u for $a_P + b_P z$, which gives $dz = \frac{du}{b_P}$, and changing the limits, $h_1 \rightarrow a_P + b_P h_1$ and $h_2 \rightarrow a_P + b_P h_2$, we obtain

$$\begin{aligned}
\left(\frac{1}{c_{1111}} \right)^{-1} &= (h_2 - h_1) \left(\int_{a_P + b_P h_1}^{a_P + b_P h_2} u^{-2} \frac{du}{b_P} \right)^{-1} = (h_2 - h_1) \left(\frac{-u^{-1}}{b_P} \Big|_{a_P + b_P h_1}^{a_P + b_P h_2} \right)^{-1} \\
&= (h_2 - h_1) (-b_P) \left((a_P + b_P h_2)^{-1} - (a_P + b_P h_1)^{-1} \right)^{-1} \\
&= (a_P + b_P h_1) (a_P + b_P h_2). \quad (7)
\end{aligned}$$

For the last term in parameter (3a),

$$\left(\frac{4(c_{1111} - c_{2323})c_{2323}}{c_{1111}} \right) = \frac{4}{h_2 - h_1} \left(\int_{h_1}^{h_2} (a_S + b_S z)^2 dz - \int_{h_1}^{h_2} \frac{(a_S + b_S z)^4}{(a_P + b_P z)^2} dz \right) = \frac{4}{h_2 - h_1} (I_2 - I_3), \quad (8)$$

where

$$I_2 = \int_{h_1}^{h_2} (a_S + b_S z)^2 dz = \frac{1}{3} (h_2 - h_1) (3 a_S^2 + 3 a_S b_S (h_1 + h_2) + b_S^2 (h_1^2 + h_1 h_2 + h_2^2)) \quad (9)$$

and

$$\begin{aligned}
I_3 = \int_{h_1}^{h_2} \frac{(a_S + b_S z)^4}{(a_P + b_P z)^2} dz = & h_2 \left(\frac{2a_P \left(\frac{2a_P b_S^4}{b_P^3} - \frac{4a_S b_S^3}{b_P^2} \right)}{b_P} - \frac{a_P^2 b_S^4}{b_P^4} + \frac{6a_S^2 b_S^2}{b_P^2} \right) \\
& - h_1 \left(\frac{2a_P \left(\frac{2a_P b_S^4}{b_P^3} - \frac{4a_S b_S^3}{b_P^2} \right)}{b_P} - \frac{a_P^2 b_S^4}{b_P^4} + \frac{6a_S^2 b_S^2}{b_P^2} \right) \\
& + h_1^2 \left(\frac{a_P b_S^4}{b_P^3} - \frac{2a_S b_S^3}{b_P^2} \right) - h_2^2 \left(\frac{a_P b_S^4}{b_P^3} - \frac{2a_S b_S^3}{b_P^2} \right) \\
& + \frac{\ln(a_P + h_1 b_P) (4a_P^3 b_S^4 - 12a_P^2 a_S b_P b_S^3 + 12a_P a_S^2 b_P^2 b_S^2 - 4a_S^3 b_P^3 b_S)}{b_P^5} \\
& - \frac{\ln(a_P + h_2 b_P) (4a_P^3 b_S^4 - 12a_P^2 a_S b_P b_S^3 + 12a_P a_S^2 b_P^2 b_S^2 - 4a_S^3 b_P^3 b_S)}{b_P^5} \\
& - \frac{h_1^3 b_S^4}{3b_P^2} + \frac{h_2^3 b_S^4}{3b_P^2} \\
& + \frac{a_P^4 b_S^4 - 4a_P^3 a_S b_P b_S^3 + 6a_P^2 a_S^2 b_P^2 b_S^2 - 4a_P a_S^3 b_P^3 b_S + a_S^4 b_P^4}{b_P (h_1 b_P^5 + a_P b_P^4)} \\
& - \frac{a_P^4 b_S^4 - 4a_P^3 a_S b_P b_S^3 + 6a_P^2 a_S^2 b_P^2 b_S^2 - 4a_P a_S^3 b_P^3 b_S + a_S^4 b_P^4}{b_P (h_2 b_P^5 + a_P b_P^4)}. \quad (10)
\end{aligned}$$

The first two terms in parameter (3b) are given by formulæ (5) and (7), whereas the third term is

$$\left(\frac{2(c_{1111} - 2c_{2323})c_{2323}}{c_{1111}} \right) = \frac{2}{h_2 - h_1} \left(\int_{h_1}^{h_2} (a_S + b_S z)^2 dz - 2 \int_{h_1}^{h_2} \frac{(a_S + b_S z)^4}{(a_P + b_P z)^2} dz \right) = \frac{2}{h_2 - h_1} (I_2 - 2I_3), \quad (11)$$

where I_2 and I_3 are given by integration constants (9) and (10). Finally, in a manner similar to obtaining the second term in parameter (3a), we use u substitution and change limits of integration to obtain the term in parameter (3e), where

$$\begin{aligned}
\left(\frac{1}{c_{2323}} \right)^{-1} &= \left(\frac{1}{h_2 - h_1} \int_{h_1}^{h_2} \frac{1}{(a_S + b_S z)^2} dz \right)^{-1} = (h_2 - h_1) \left(\int_{h_1}^{h_2} (a_S + b_S z)^{-2} dz \right)^{-1} \\
&= (a_S + b_S h_1) (a_S + b_S h_2). \quad (12)
\end{aligned}$$

Thus, using formulæ (4), (5), (7), (8), (11), (12), along with integration constants (6), (9), (10), we may

restate Backus parameters (3a)–(3f) as

$$c_{1111}^{\overline{\text{II}}}(h_1, h_2, a_S, b_S, a_P, b_P) = \left(1 - \frac{2I_1}{h_2 - h_1}\right)^2 (a_P + b_P h_1)(a_P + b_P h_2) + \frac{4}{h_2 - h_1}(I_2 - I_3), \quad (13a)$$

$$c_{1122}^{\overline{\text{II}}}(h_1, h_2, a_S, b_S, a_P, b_P) = \left(1 - \frac{2I_1}{h_2 - h_1}\right)^2 (a_P + b_P h_1)(a_P + b_P h_2) + \frac{2}{h_2 - h_1}(I_2 - 2I_3), \quad (13b)$$

$$c_{1133}^{\overline{\text{II}}}(h_1, h_2, a_S, b_S, a_P, b_P) = \left(1 - \frac{2I_1}{h_2 - h_1}\right) (a_P + b_P h_1)(a_P + b_P h_2), \quad (13c)$$

$$c_{1212}^{\overline{\text{II}}}(h_1, h_2, a_S, b_S) = \frac{1}{3} (3a_S^2 + 3a_S b_S (h_1 + h_2) + b_S^2 (h_1^2 + h_1 h_2 + h_2^2)), \quad (13d)$$

$$c_{2323}^{\overline{\text{II}}}(h_1, h_2, a_S, b_S) = (a_S + b_S h_1)(a_S + b_S h_2), \quad (13e)$$

$$c_{3333}^{\overline{\text{II}}}(h_1, h_2, a_P, b_P) = (a_P + b_P h_1)(a_P + b_P h_2). \quad (13f)$$

2.2 Anisotropy parameters

The anisotropy of any transversely isotropic medium may be described by the Thomsen (1986) parameters. Thus, using Backus parameters (13), we define

$$\gamma = \gamma(h_1, h_2, a_S, b_S) := \frac{c_{1212}^{\overline{\text{II}}} - c_{2323}^{\overline{\text{II}}}}{2c_{2323}^{\overline{\text{II}}}}, \quad (14a)$$

$$\delta = \delta(h_1, h_2, a_S, b_S, a_P, b_P) := \frac{\left(c_{1133}^{\overline{\text{II}}} + c_{2323}^{\overline{\text{II}}}\right)^2 - \left(c_{3333}^{\overline{\text{II}}} - c_{2323}^{\overline{\text{II}}}\right)^2}{2c_{3333}^{\overline{\text{II}}}\left(c_{3333}^{\overline{\text{II}}} - c_{2323}^{\overline{\text{II}}}\right)}, \quad (14b)$$

$$\varepsilon = \varepsilon(h_1, h_2, a_S, b_S, a_P, b_P) := \frac{c_{1111}^{\overline{\text{II}}} - c_{3333}^{\overline{\text{II}}}}{2c_{3333}^{\overline{\text{II}}}}. \quad (14c)$$

Explicitly, parameter (14a) is

$$\gamma = \gamma(h_1, h_2, a_S, b_S) = \frac{b_S^2 (h_1 - h_2)^2}{6(a_S + b_S h_1)(a_S + b_S h_2)}. \quad (15a)$$

For parameter (14b),

$$\begin{aligned} \delta &= \delta(h_1, h_2, a_S, b_S, a_P, b_P) \\ &= \frac{2\delta_{k1}(-b_P(h_1 - h_2)(2a_P + b_P(h_1 + h_2)) + \delta_{k2})(b_P(h_1 - h_2)\delta_{k3} + \delta_{k1}\delta_{k2})}{b_P^6(a_P + b_P h_1)(h_1 - h_2)^2(a_P + b_P h_2)(a_P^2 + \delta_{k4} + a_P b_P(h_1 + h_2) - a_S b_S(h_1 + h_2))}, \end{aligned} \quad (15b)$$

where

$$\begin{aligned} \delta_{k1} &= b_S(-a_S b_P + a_P b_S), \\ \delta_{k2} &= 2(a_P + b_P h_1)(a_P + b_P h_2) \ln\left(\frac{a_P + b_P h_1}{a_P + b_P h_2}\right), \\ \delta_{k3} &= (a_P^2(b_P^2 - 2b_S^2) + b_P^2(\delta_{k4}) + a_P b_P(2a_S b_S + (b_P - b_S)(b_P + b_S)(h_1 + h_2))), \\ \delta_{k4} &= -a_S^2 + (b_P - b_S)(b_P + b_S)h_1 h_2. \end{aligned}$$

For parameter (14c),

$$\varepsilon = \varepsilon(h_1, h_2, a_S, b_S, a_P, b_P) = \frac{2b_S\left(b_P^3(h_1 - h_2)^2(-6a_P^2 b_P b_S + b_P(\varepsilon_{k1}) + 3a_P(\varepsilon_{k2})) + (\varepsilon_{k3})(\varepsilon_{k4})\right)}{3b_P^6(a_P + b_P h_1)(h_1 - h_2)^2(a_P + b_P h_2)} \quad (15c)$$

where

$$\begin{aligned}
\varepsilon_{k1} &= -12 a_S^2 b_S + (b_P - b_S) b_S (b_P + b_S) (h_1 - h_2)^2 + 3 a_S (b_P^2 - 2 b_S^2) (h_1 + h_2) , \\
\varepsilon_{k2} &= 2 a_S (b_P^2 + 2 b_S^2) + b_S (-b_P^2 + 2 b_S^2) (h_1 + h_2) , \\
\varepsilon_{k3} &= 6 (a_S b_P - a_P b_S) (a_P + b_P h_1) (a_P + b_P h_2) \ln \left(\frac{a_P + b_P h_1}{a_P + b_P h_2} \right) , \\
\varepsilon_{k4} &= -b_P (b_P^2 - 2 b_S^2) (h_1 - h_2) + 2 b_S (-a_S b_P + a_P b_S) \ln \left(\frac{a_P + b_P h_2}{a_P + b_P h_1} \right) .
\end{aligned}$$

2.3 Total differentials of anisotropy parameters

To quantify the uncertainty of expressions (15a)–(15c), i.e., the sensitivity to changes in model parameters, we require the total differential. We demonstrate this, we differentiate γ with respect to each of its coordinates directions to obtain its linear functional

$$d\gamma = \left(\frac{\partial \gamma}{\partial h_1} \right) dh_1 + \left(\frac{\partial \gamma}{\partial h_2} \right) dh_2 + \left(\frac{\partial \gamma}{\partial a_S} \right) da_S + \left(\frac{\partial \gamma}{\partial b_S} \right) db_S , \quad (16a)$$

where

$$\begin{aligned}
\frac{\partial \gamma}{\partial h_1} &= \frac{b_S^2 (h_1 - h_2) (2 a_S + b_S (h_1 + h_2))}{6 (a_S + b_S h_1)^2 (a_S + b_S h_2)} , \\
\frac{\partial \gamma}{\partial h_2} &= -\frac{b_S^2 (h_1 - h_2) (2 a_S + b_S (h_1 + h_2))}{6 (a_S + b_S h_1) (a_S + b_S h_2)^2} , \\
\frac{\partial \gamma}{\partial a_S} &= -\frac{b_S^2 (h_1 - h_2)^2 (2 a_S + b_S (h_1 + h_2))}{6 (a_S + b_S h_1)^2 (a_S + b_S h_2)^2} , \\
\frac{\partial \gamma}{\partial b_S} &= \frac{a_S b_S (h_1 - h_2)^2 (2 a_S + b_S (h_1 + h_2))}{6 (a_S + b_S h_1)^2 (a_S + b_S h_2)^2} .
\end{aligned}$$

We may perform similar operations on δ and ε to obtain

$$d\delta = \left(\frac{\partial \delta}{\partial h_1} \right) dh_1 + \left(\frac{\partial \delta}{\partial h_2} \right) dh_2 + \left(\frac{\partial \delta}{\partial a_S} \right) da_S + \left(\frac{\partial \delta}{\partial b_S} \right) db_S + \left(\frac{\partial \delta}{\partial a_P} \right) da_P + \left(\frac{\partial \delta}{\partial b_P} \right) db_P \quad (16b)$$

and

$$d\varepsilon = \left(\frac{\partial \varepsilon}{\partial h_1} \right) dh_1 + \left(\frac{\partial \varepsilon}{\partial h_2} \right) dh_2 + \left(\frac{\partial \varepsilon}{\partial a_S} \right) da_S + \left(\frac{\partial \varepsilon}{\partial b_S} \right) db_S + \left(\frac{\partial \varepsilon}{\partial a_P} \right) da_P + \left(\frac{\partial \varepsilon}{\partial b_P} \right) db_P . \quad (16c)$$

We do not list the the resultant expressions since they would require half-a-dozen pages. However, the expressions for the partial derivatives of differentials (16b) and (16c) may be derived using a symbolic software, such as Mathematica.

3 Methods for well-posedness

Expressions (15a)–(15c) form an ill-posed system of three equations with nine unknowns, where

$$\begin{cases} \gamma = \gamma (h_1, h_2, a_S, b_S) \\ \delta = \delta (h_1, h_2, a_S, b_S, a_P, b_P) \\ \varepsilon = \varepsilon (h_1, h_2, a_S, b_S, a_P, b_P) \end{cases} . \quad (17)$$

We use differentials (16a)–(16c) to form a measure of error. To obtain solutions, we require well-posedness, which necessitates information for six of the nine unknown parameters. Using the Backus average on a region of interest of a well log, we reduce the number of unknowns to four. In particular, we specify h_1 and h_2 , and calculate values for $\gamma =: \gamma^{\overline{\text{PI}}}$, $\delta =: \delta^{\overline{\text{PI}}}$, $\varepsilon =: \varepsilon^{\overline{\text{PI}}}$, where $\overline{\text{PI}}$ denotes a quantity obtained using the Backus (1962) average. Information for any of a_S, b_S, a_P, b_P must be obtained using additional methods.

To obtain information for the remaining model parameters, we use 1-D tomography and the *ab* model.

3.1 1-D tomography

To obtain linear inhomogeneity parameters from VSP data, we use a 1-D tomography method. The inversion algorithm, therein, is based on the Levenberg-Marquardt least-square solution. As a result of inversion, we obtain a velocity profile corresponding to discrete depths. The inverted velocity profile represents the velocity of a vertically inhomogeneous medium. To calculate the linear inhomogeneity parameters for a particular region, we apply the linear regression to the resultant velocities for the required depths. The 1-D tomography can provide relatively good results in the case of a better initial model, a sufficient number of data, and that the assumption of linear inhomogeneity holds firmly for the medium.

3.2 *ab* model

The *ab* model is a travelttime inversion method. In this method, the velocity model is a linear function of depth. To obtain the travelttime in a depth segment from borehole velocity, we assume the medium is composed of multiple thin isotropic layers. Based on that assumption, we calculate Fermat’s travelttime. In general, the borehole data contains high-frequency contents, which restricts the ray to travel from a source to a receiver with high offset. To synthesize sufficient travelttime data, we need travelttime for both near and high offsets. That is possible only if we remove the higher frequencies from the data. We apply a weighted average in every twelve consecutive data points to filter out those contents. As an outcome, we get a smoother velocity, which allows rays to travel from source to receiver with sufficiently more significant offset. In the inversion, we minimize the difference between the Fermat’s travelttime and the model travelttime (Slawinski and Slawinski, 1999) and obtain linear inhomogeneity parameters.

3.3 Mizzen O-16

The VSP and well log data used, herein, was obtained from the Mizzen O-16 discovery well, which is a site in the Flemish Pass basin and was drilled in 2009 by Statoil (Enachescu, 2011). The well log data used is supplied by IHS energy; the data description is provided in Ikon Science and Nalcor Energy (2016). We use *P*- and *S*-wavespeed measurements for depths of at depth 1865m to 2648.60 m.

The checkshot (VSP) data is provided by the Canada-Newfoundland & Labrador Offshore Petroleum Board (C-NLOPB). Therein, the travelttime data corresponds to a single source and multiple receivers. The source is located at a 26.5 m offset and the receivers are placed along vertical axis, starting at depth 1865 m and ending at 2650 m. We consider our last receiver at depth 2650m so that the velocity inversion from travelttime merges with the region where the well log data are recorded. The descriptions of the data are given in Tables 1 and 2, which are collected with the permission of the Petroleum Development Section of Natural Resources, Government of Newfoundland and Labrador.

Field	Well	KB (m)	TVD (m)	Water depth (m)	Spud date	Log data
Mizzen	O-16	21.15	3797	1095	2008	✓

Table 1: Description of the well for log data

Field	Well	Offset (m)	TVD (m)	Water depth (m)	Spud date	Checkshot
Mizzen	O-16	26.50	3797	1095	2009	✓

Table 2: Description of the well for checkshot data

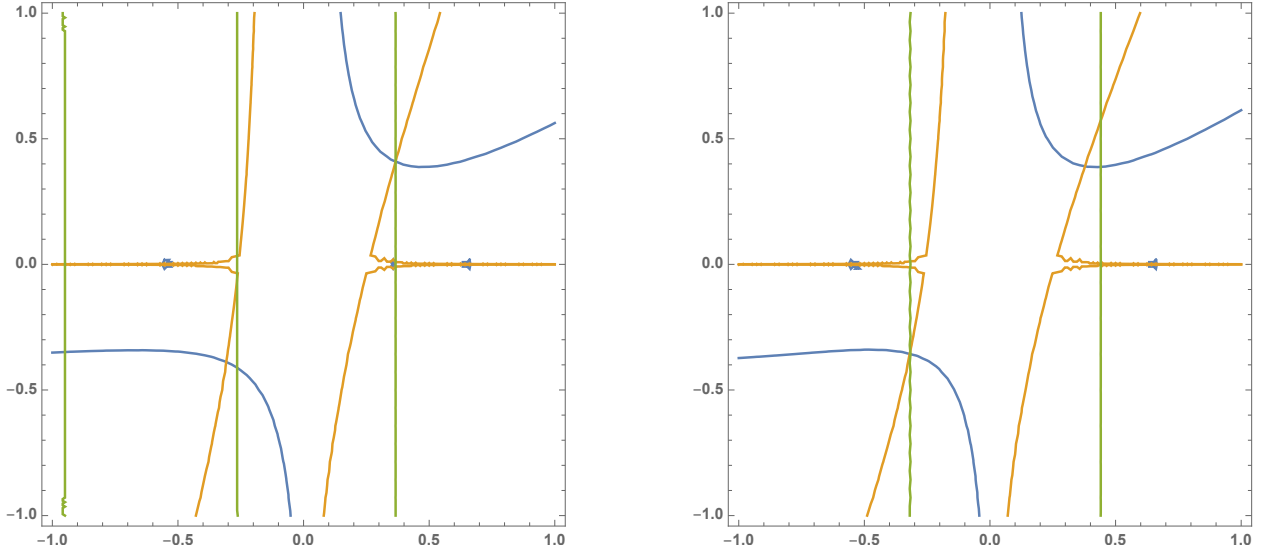


Figure 1: Contour plot of anisotropy values (18), where b_P is along the vertical axis and b_S is along the horizontal axis. Green lines represent $\gamma = \gamma^{\overline{\text{TI}}}$; orange lines represents $\delta = \delta^{\overline{\text{TI}}}$, blue lines represent $\varepsilon = \varepsilon^{\overline{\text{TI}}}$.

4 Numerical search

4.1 Restrictions

In our numerical search, we have two restrictions. First, the stability conditions of isotropy restrict the values for a_S and a_P such that

$$a_P > 2a_S / \sqrt{3}.$$

Second, to remain consistent with the assumption of constantly increasing velocity gradient with depth of Slawinski and Slawinski (1999), we restrict our solutions to positive values of b_P and b_S . However, it is worth noting that there do exist solutions for negative values of b_P and b_S .

We may demonstrate this with a numerical example. For, say, an input of $a_P = 2040.36 \text{ ms}^{-1}$, there exist two solutions, as illustrated by the two instances of triple-point intersection in the left- and right-hand plots of Figure 1. Therein, the left-hand plot corresponds to a solution of positive b_P and b_S , where

$$a_S = 752.95 \text{ ms}^{-1}, \quad b_S = 0.3666 \text{ s}^{-1}, \quad a_P = 2164.68 \text{ ms}^{-1}, \quad b_P = 0.4081 \text{ s}^{-1}.$$

However, the right-hand plot corresponds to a solution of negative b_P and b_S , where

$$a_S = 906.32 \text{ ms}^{-1}, \quad b_S = -0.3194 \text{ s}^{-1}, \quad a_P = 2164.68 \text{ ms}^{-1}, \quad b_P = -0.3556 \text{ s}^{-1}.$$

Throughout the entirety of the numerical results, we consider positive solutions only.

4.2 Calculations

Let us obtain a solution to system (17) using the methodology of Section 3.1 with the VSP data of Mizzen O-16. Using results from 1-D tomography on traveltimes data, we recover a velocity profile as a function of

depth. For a region of interest, whose depth ranges from 1865 m to 2648.60 m, we recover two parameters, namely a_P and b_P . We may use either parameter as input to system (17) to obtain values for the remaining three unknowns.

For example, we use $a_{P_{VSP,in}} = 1415 \text{ ms}^{-1}$ and $b_{P_{VSP,in}} = 0.70 \text{ s}^{-1}$ as startup values for the tomography. For the region of interest, we recover $a_{P_{VSP,out}} = 1354.9 \text{ ms}^{-1}$ and $b_{P_{VSP,out}} = 0.3933 \text{ s}^{-1}$, where, at the top of the region, $a_{P_{\text{layer}}} = a_{P_{VSP,out}} + b_{P_{VSP,out}} \cdot 1865 \text{ m} = 2088.38 \text{ ms}^{-1}$. We input $b_P = b_{P_{VSP,out}}$ into system (17), for

$$h_1 = 0 \text{ m}, \quad h_2 = (2648.6 - 1865) \text{ m} = 783.6 \text{ m},$$

$$\gamma^{\overline{\text{II}}} = 0.017561151400350, \quad \delta^{\overline{\text{II}}} = -0.005822848520484, \quad \varepsilon^{\overline{\text{II}}} = 0.002868244418444, \quad (18)$$

and obtain

$$a_S = 725.55 \text{ ms}^{-1}, \quad b_S = 0.3533 \text{ s}^{-1}, \quad a_P = 2085.91 \text{ ms}^{-1}, \quad b_P = 0.3933 \text{ s}^{-1}. \quad (19)$$

It is clear that $a_{P_{\text{layer}}} \neq a_P$ but we may perform an error analysis to assess the ‘‘closeness’’ of our result. To do so, we recall expressions (16a), (16b), (16c), which are total differentials $d\gamma, d\delta, d\varepsilon$. Using uncertainty measures for parameters (19), where

$$dh_1 = dh_2 = 0.05 \text{ m}, \quad da_S = da_P = 2 \text{ ms}^{-1}, \quad db_S = db_P = 0.01 \text{ s}^{-1}, \quad (20)$$

we obtain

$$d\gamma = 0.000790010132156, \quad d\delta = -0.000299948944243, \quad d\varepsilon = 0.000143889902574. \quad (21)$$

We obtain a new set of solutions for the lower limit of anisotropy by subtracting values (21) from the left-hand sides of system (17), which are

$$a_{S_-} = 742.47 \text{ ms}^{-1}, \quad b_{S_-} = 0.3522 \text{ s}^{-1}, \quad a_{P_-} = 2138.75 \text{ ms}^{-1}, \quad b_P = 0.3933 \text{ s}^{-1}. \quad (22)$$

Similarly, the upper limit of anisotropy is obtained adding values (21), which results in

$$a_{S_+} = 709.58 \text{ ms}^{-1}, \quad b_{S_+} = 0.354246 \text{ s}^{-1}, \quad a_{P_+} = 2036.58 \text{ ms}^{-1}, \quad b_P = 0.3933 \text{ s}^{-1}. \quad (23)$$

Thus, we find that $a_{P_{\text{layer}}}$ falls within the range determined by a_{P_-} and a_{P_+} . In particular, such startup values provide results that are within 0.12% and 0.13%, respectively, of the theoretical predictions. We may repeat this entire process using $a_P = a_{P_{VSP,out}}$ as input. In addition, this process may be repeated for a range of VSP startup values, in order to find the combination of startup values that are closest to the predicted model parameters indicated by the analytical relation. We tabulate the results of such a process, for values of $a_{P_{VSP,in}}$ ranging from 1325 ms^{-1} to 1515 ms^{-1} , with increments of 20 ms^{-1} , and $b_{P_{VSP,in}}$ ranging from 0.57 s^{-1} to 0.7 s^{-1} , with increments of 0.01 s^{-1} , in Table 3 of Appendix A.

To compare the results from VSP with the ab model, we repeat this process for the same range of values of $a_{P_{ab,in}}$ and $b_{P_{ab,in}}$. The results are tabulated in Table 4 of Appendix A. In comparison, the startup values of $a_{P_{ab,in}} = 1625 \text{ ms}^{-1}$ and $b_{P_{ab,in}} = 0.6 \text{ s}^{-1}$, provide results that are within 0.03% and 0.03%, respectively, of the theoretical predictions.

We illustrate the entirety of the results of Tables 3 and 4 in Figures 2a and 2b. Therein, the solid red line represents the solution to system (17) corresponding to the value on the horizontal axis, and the solid black lines represent solutions for the lower and upper limits of anisotropy, corresponding to uncertainty parameters (20). Orange diamonds represent the solutions from 1-D tomography and blue dots represent solutions from the ab model.

5 Discussion

For each solution method, we obtain some $a_{P_{VSP,ab}}$ and $b_{P_{VSP,ab}}$ parameter. Using the outputted $a_{P_{VSP,ab}}$ as input to system (17), we calculate b_P, b_{P_-}, b_{P_+} , and compare them to the outputted $b_{P_{VSP,ab}}$. These

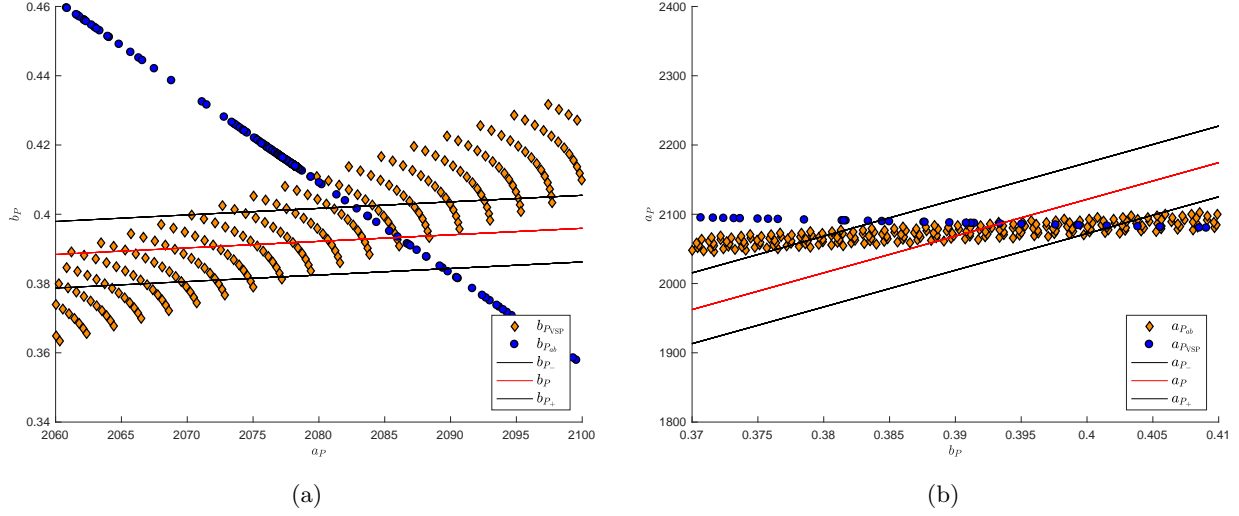


Figure 2: Solutions of 1-D tomography and ab -model for startup values of $a_{P_{VSP},in}$ and $b_{P_{VSP},in}$ in Table with VSP results and $a_{P_{ab},in}$ and $b_{P_{ab},in}$ in Table with ab results.

results are illustrated in Figure 2a; the opposite operation is performed and those results are illustrated in Figure 2b.

In both subplots of Figure 2, we observe that the area of solutions for 1-D tomography overlaps the line of ab -model solutions. To discern which startup values lead to common outputs, we turn our attention to Figure 3. Therein, startup values of $a_{P_{VSP},in} = 1415 \text{ ms}^{-1}$ and $b_{P_{VSP},in} = 0.7 \text{ ms}^{-1}$ result in $a_{P_{VSP},out} = 2088.38 \text{ ms}^{-1}$ and $b_{P_{VSP},out} = 0.3932 \text{ ms}^{-1}$. These results, as stated in Section 4.2, are within 0.12% and 0.13%, respectively, of the theoretical predictions. Similarly, startup values of $a_{P_{ab},in} = 1625 \text{ ms}^{-1}$ and $b_{P_{ab},in} = 0.6 \text{ ms}^{-1}$ result in outputs that are within 0.03% of the theoretical predictions.

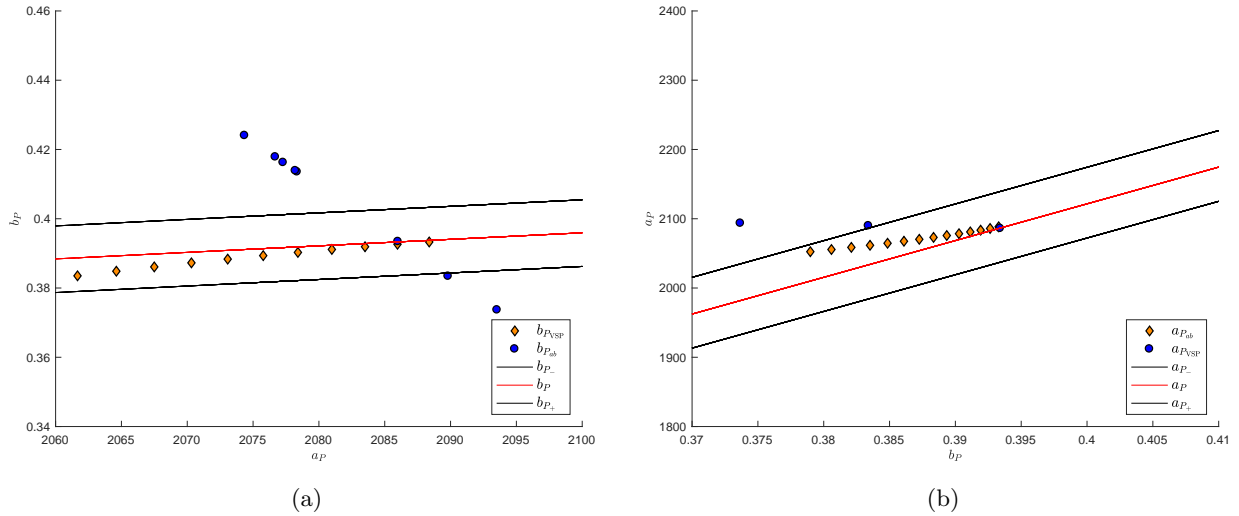


Figure 3: Solutions of 1-D tomography and ab -model for startup values of $a_{P_{VSP},in} = 1415 \text{ ms}^{-1}$ and $b_{P_{VSP},in}$ incrementing by 0.01 s^{-1} from 0.57 s^{-1} to 0.7 s^{-1} , and $a_{P_{ab},in} = 1625 \text{ ms}^{-1}$ and $b_{P_{ab},in}$ incrementing by 0.05 s^{-1} from 0.25 s^{-1} to 0.65 s^{-1} .

6 Conclusion and future work

In this article, we show that we can obtain multiple solution from VSP and *ab*-model that do not lie in the theoretical range. However, we also show that there exist some common solution.

Based on the initial model, we find that there are some initial values that lead to that common solution, which may allow us to conclude that, by tuning initial model parameters, we can obtain the common solution set.

The number of traveltime data from the field measurement plays an important role in the VSP method. As a future work, we plan to apply the analytical relation and seismic methods to a site that possesses more data, which may produces a stable solution for different initial models in the VSP method.

By far, we have shown that the relationship between inhomogeneity and anisotropy provides reasonable solution in compare to the seismic methods. In addition to our future project, we wish to examine the limitation of the analytical relationship by calculating Backus average from a sparse well log data.

References

- Backus, G. E. (1962). Long-wave elastic anisotropy produced by horizontal layering. *Journal of Geophysical Research*, 67(11):4427–4440.
- C-NLOPB. Canada-Newfoundland & Labrador Offshore Petroleum Board website. <https://www.cnlopb.ca>.
- Enachescu, M. E. (2011). Petroleum exploration opportunities in area “C” - Flemish pass/North Central Ridge: Calls for bids NL11-02. URL: https://www.nr.gov.nl.ca/nr/invest/enachescu_NL1102Flemish.pdf.
- Ikon Science and Nalcor Energy (2016). Regional rock physics analysis of offshore Newfoundland and Labrador: Unlocking the shelf-to-deep-transition. <http://exploration.nalcorenergy.com/wp-content/uploads/2017/01/RockPhysics.pdf>.
- Slawinski, M. A. (2018). *Waves and rays in seismology: Answers to unasked questions*. World Scientific, 2nd edition.
- Slawinski, R. A. and Slawinski, M. A. (1999). On raytracing in constant velocity-gradient media: Calculus approach. *Canadian Journal of Exploration Geophysics*, 35(1/2):24–27.
- Slotnick, M. M. (1959). *Lessons in seismic computing*. Society of Explorational Geophysicists.
- Thomsen, L. (1986). Weak elastic anisotropy. *Geophysics*, 51(10):1954–1966.

A Tables

Table 3: VSP results

Startup values		VSP results		Using $b_{P_{VSP,out}}$ as input				Using $a_{P_{layer}}$ as input			
$a_{P_{VSP,in}}$	$b_{P_{VSP,in}}$	$a_{P_{VSP,out}}$	$b_{P_{VSP,out}}$	$a_{P_{layer}}$	a_{P_+}	a_P	a_{P_-}	$b_{P_{VSP,out}}$	b_{P_-}	b_P	b_{P_+}
1320.0	0.57	1292.3	0.4317	2097.42	2240.18	2289.65	2342.32	0.4317	0.3857	0.3955	0.405
1325.0	0.57	1295.46	0.4286	2094.83	2223.84	2273.3	2325.98	0.4286	0.3853	0.395	0.4045
1330.0	0.57	1298.58	0.4256	2092.27	2207.69	2257.14	2309.83	0.4256	0.3848	0.3945	0.404
1335.0	0.57	1301.65	0.4226	2089.73	2191.74	2241.18	2293.89	0.4226	0.3843	0.394	0.4035
1340.0	0.57	1304.68	0.4196	2087.22	2175.98	2225.41	2278.13	0.4196	0.3838	0.3935	0.4031
1345.0	0.57	1307.68	0.4167	2084.74	2160.42	2209.84	2262.57	0.4167	0.3834	0.3931	0.4026
1350.0	0.57	1310.63	0.4138	2082.28	2145.04	2194.45	2247.19	0.4138	0.3829	0.3926	0.4021
1355.0	0.57	1313.54	0.4109	2079.84	2129.85	2179.25	2232.0	0.4109	0.3824	0.3921	0.4017
1360.0	0.57	1316.41	0.4081	2077.43	2114.83	2164.22	2216.99	0.4081	0.382	0.3917	0.4012
1365.0	0.57	1319.24	0.4053	2075.04	2100.0	2149.37	2202.16	0.4053	0.3815	0.3912	0.4008
1370.0	0.57	1322.04	0.4025	2072.68	2085.33	2134.7	2187.49	0.4025	0.3811	0.3908	0.4003
1375.0	0.57	1324.8	0.3998	2070.34	2070.85	2120.2	2173.01	0.3998	0.3806	0.3904	0.3999
1380.0	0.57	1327.52	0.3971	2068.02	2056.53	2105.87	2158.69	0.3971	0.3802	0.3899	0.3994
1385.0	0.57	1330.21	0.3944	2065.73	2042.37	2091.7	2144.54	0.3944	0.3798	0.3895	0.399
1390.0	0.57	1332.86	0.3917	2063.45	2028.38	2077.7	2130.55	0.3917	0.3793	0.3891	0.3986

1765.0	0.4	2076.36	2272.86	2220.14	2170.71	0.4186	0.401	0.3915	0.3818
1785.0	0.4	2076.22	2274.8	2222.08	2172.65	0.419	0.401	0.3915	0.3817
1805.0	0.4	2076.07	2276.82	2224.1	2174.67	0.4193	0.401	0.3914	0.3817
1005.0	0.45	2078.35	2246.05	2193.3	2143.89	0.4135	0.4014	0.3919	0.3821
1025.0	0.45	2078.1	2249.36	2196.62	2147.21	0.4142	0.4013	0.3918	0.3821
1045.0	0.45	2078.28	2246.95	2194.2	2144.79	0.4137	0.4014	0.3918	0.3821
1065.0	0.45	2078.34	2246.09	2193.34	2143.93	0.4135	0.4014	0.3919	0.3821
1085.0	0.45	2078.35	2246.05	2193.3	2143.89	0.4135	0.4014	0.3919	0.3821
1105.0	0.45	2078.1	2249.42	2196.68	2147.27	0.4142	0.4013	0.3918	0.3821
1125.0	0.45	2078.28	2246.98	2194.23	2144.82	0.4137	0.4014	0.3918	0.3821
1145.0	0.45	2078.34	2246.14	2193.39	2143.98	0.4136	0.4014	0.3919	0.3821
1165.0	0.45	2078.28	2246.98	2194.24	2144.83	0.4137	0.4014	0.3918	0.3821
1185.0	0.45	2078.34	2246.14	2193.39	2143.98	0.4136	0.4014	0.3919	0.3821
1205.0	0.45	2078.34	2246.13	2193.39	2143.98	0.4136	0.4014	0.3919	0.3821
1225.0	0.45	2074.25	2302.98	2250.28	2200.84	0.4243	0.4006	0.3911	0.3814
1245.0	0.45	2076.4	2272.97	2220.24	2170.82	0.4186	0.401	0.3915	0.3818
1265.0	0.45	2075.48	2285.83	2233.11	2183.68	0.421	0.4008	0.3913	0.3816
1285.0	0.45	2074.51	2299.51	2246.8	2197.36	0.4236	0.4007	0.3911	0.3814
1305.0	0.45	2073.84	2308.8	2256.1	2206.65	0.4254	0.4005	0.391	0.3813
1325.0	0.45	2073.58	2312.46	2259.77	2210.32	0.4261	0.4005	0.391	0.3812
1345.0	0.45	2073.67	2311.21	2258.51	2209.06	0.4258	0.4005	0.391	0.3813
1365.0	0.45	2074.03	2306.24	2253.54	2204.09	0.4249	0.4006	0.391	0.3813
1385.0	0.45	2074.57	2298.66	2245.96	2196.51	0.4235	0.4007	0.3912	0.3814
1405.0	0.45	2075.24	2289.3	2236.58	2187.15	0.4217	0.4008	0.3913	0.3816
1425.0	0.45	2076.0	2278.75	2226.03	2176.6	0.4197	0.4009	0.3914	0.3817
1445.0	0.45	2076.81	2267.42	2214.69	2165.27	0.4176	0.4011	0.3916	0.3819
1465.0	0.45	2077.66	2255.6	2202.86	2153.45	0.4153	0.4013	0.3917	0.382
1485.0	0.45	2078.53	2243.49	2190.74	2141.33	0.4131	0.4014	0.3919	0.3822
1505.0	0.45	2079.41	2231.21	2178.45	2129.05	0.4107	0.4016	0.3921	0.3823
1525.0	0.45	2078.34	2246.19	2193.44	2144.04	0.4136	0.4014	0.3919	0.3821
1545.0	0.45	2078.32	2246.37	2193.63	2144.22	0.4136	0.4014	0.3919	0.3821
1565.0	0.45	2078.3	2246.63	2193.88	2144.48	0.4136	0.4014	0.3919	0.3821
1585.0	0.45	2078.28	2246.96	2194.21	2144.8	0.4137	0.4014	0.3918	0.3821
1605.0	0.45	2078.25	2247.35	2194.6	2145.2	0.4138	0.4014	0.3918	0.3821
1625.0	0.45	2078.22	2247.81	2195.07	2145.66	0.4139	0.4014	0.3918	0.3821
1645.0	0.45	2078.18	2248.34	2195.59	2146.19	0.414	0.4014	0.3918	0.3821
1665.0	0.45	2078.13	2248.93	2196.19	2146.78	0.4141	0.4013	0.3918	0.3821
1685.0	0.45	2078.08	2249.59	2196.84	2147.43	0.4142	0.4013	0.3918	0.3821
1705.0	0.45	2078.03	2250.31	2197.56	2148.15	0.4143	0.4013	0.3918	0.3821
1725.0	0.45	2077.97	2251.07	2198.33	2148.92	0.4145	0.4013	0.3918	0.3821
1745.0	0.45	2077.91	2251.92	2199.17	2149.76	0.4146	0.4013	0.3918	0.3821
1765.0	0.45	2077.85	2252.8	2200.06	2150.65	0.4148	0.4013	0.3918	0.3821
1785.0	0.45	2077.78	2253.75	2201.01	2151.59	0.415	0.4013	0.3918	0.382
1805.0	0.45	2077.7	2254.75	2202.01	2152.6	0.4152	0.4013	0.3917	0.382
1005.0	0.5	2078.0	2250.75	2198.01	2148.6	0.4144	0.4013	0.3918	0.3821
1025.0	0.5	2078.23	2247.58	2194.84	2145.43	0.4138	0.4014	0.3918	0.3821
1045.0	0.5	2078.33	2246.29	2193.55	2144.14	0.4136	0.4014	0.3919	0.3821
1065.0	0.5	2078.23	2247.59	2194.85	2145.44	0.4138	0.4014	0.3918	0.3821
1085.0	0.5	2078.33	2246.3	2193.55	2144.14	0.4136	0.4014	0.3919	0.3821
1105.0	0.5	2078.0	2250.78	2198.04	2148.63	0.4144	0.4013	0.3918	0.3821
1125.0	0.5	2077.01	2264.06	2211.33	2161.91	0.4169	0.4011	0.3916	0.3819
1145.0	0.5	2078.13	2248.96	2196.21	2146.81	0.4141	0.4013	0.3918	0.3821
1165.0	0.5	2078.03	2250.35	2197.61	2148.2	0.4143	0.4013	0.3918	0.3821
1185.0	0.5	2077.9	2252.13	2199.39	2149.98	0.4147	0.4013	0.3918	0.3821
1205.0	0.5	2074.27	2302.64	2249.94	2200.49	0.4242	0.4006	0.3911	0.3814
1225.0	0.5	2062.99	2460.21	2407.62	2358.08	0.4539	0.3985	0.389	0.3792
1245.0	0.5	2062.17	2471.72	2419.15	2369.59	0.4561	0.3983	0.3888	0.3791
1265.0	0.5	2061.76	2477.48	2424.9	2375.35	0.4572	0.3983	0.3887	0.379
1285.0	0.5	2061.68	2478.6	2426.03	2376.47	0.4574	0.3982	0.3887	0.379
1305.0	0.5	2061.85	2476.13	2423.56	2374.01	0.457	0.3983	0.3888	0.379
1325.0	0.5	2062.23	2470.96	2418.38	2368.83	0.456	0.3983	0.3888	0.3791
1345.0	0.5	2062.74	2463.75	2411.17	2361.62	0.4546	0.3984	0.3889	0.3792
1365.0	0.5	2063.37	2455.03	2402.44	2352.9	0.453	0.3986	0.389	0.3793
1385.0	0.5	2064.07	2445.21	2392.61	2343.08	0.4511	0.3987	0.3892	0.3795
1405.0	0.5	2076.75	2268.1	2215.38	2165.95	0.4177	0.4011	0.3916	0.3818
1425.0	0.5	2076.91	2265.91	2213.18	2163.76	0.4173	0.4011	0.3916	0.3819
1445.0	0.5	2077.07	2263.68	2210.95	2161.53	0.4169	0.4011	0.3916	0.3819
1465.0	0.5	2077.23	2261.48	2208.74	2159.32	0.4164	0.4012	0.3917	0.3819
1485.0	0.5	2077.38	2259.34	2206.61	2157.19	0.416	0.4012	0.3917	0.382
1505.0	0.5	2077.53	2257.31	2204.57	2155.16	0.4157	0.4012	0.3917	0.382
1525.0	0.5	2077.67	2255.41	2202.67	2153.25	0.4153	0.4013	0.3917	0.382
1545.0	0.5	2077.8	2253.65	2200.91	2151.5	0.415	0.4013	0.3918	0.382
1565.0	0.5	2077.91	2252.05	2199.31	2149.9	0.4147	0.4013	0.3918	0.3821
1585.0	0.5	2078.01	2250.63	2197.89	2148.48	0.4144	0.4013	0.3918	0.3821
1605.0	0.5	2078.1	2249.39	2196.64	2147.23	0.4142	0.4013	0.3918	0.3821
1625.0	0.5	2074.36	2301.65	2248.95	2199.51	0.424	0.4006	0.3911	0.3814
1645.0	0.5	2075.22	2289.61	2236.9	2187.47	0.4218	0.4008	0.3913	0.3816
1665.0	0.5	2076.08	2277.68	2224.96	2175.53	0.4195	0.401	0.3914	0.3817
1685.0	0.5	2076.92	2265.86	2213.13	2163.71	0.4173	0.4011	0.3916	0.3819
1705.0	0.5	2077.76	2254.16	2201.42	2152.01	0.4151	0.4013	0.3918	0.382
1725.0	0.5	2078.6	2242.58	2189.83	2140.43	0.4129	0.4014	0.3919	0.3822
1745.0	0.5	2079.42	2231.13	2178.37	2128.98	0.4107	0.4016	0.3921	0.3823
1765.0	0.5	2078.34	2246.18	2193.43	2144.02	0.4136	0.4014	0.3919	0.3821
1785.0	0.5	2094.31	2023.96	1971.01	1921.77	0.3716	0.4044	0.3949	0.3852
1805.0	0.5	2098.54	1965.24	1912.22	1863.04	0.3605	0.4052	0.3957	0.386
1005.0	0.55	2077.2	2261.59	2208.86	2159.44	0.4165	0.4012	0.3916	0.3819
1025.0	0.55	2072.82	2322.87	2270.18	2220.72	0.428	0.4003	0.3908	0.3811
1045.0	0.55	2071.15	2346.18	2293.51	2244.04	0.4324	0.4	0.3905	0.3808
1065.0	0.55	2068.82	2378.74	2326.1	2276.6	0.4386	0.3996	0.3901	0.3803
1085.0	0.55	2066.33	2413.36	2360.75	2311.23	0.4451	0.3991	0.3896	0.3799
1105.0	0.55	2064.08	2444.89	2392.29	2342.76	0.4511	0.3987	0.3892	0.3795
1125.0	0.55	2062.23	2470.71	2418.13	2368.58	0.4559	0.3983	0.3888	0.3791
1145.0	0.55	2060.85	2490.01	2437.44	2387.88	0.4596	0.398	0.3886	0.3788
1165.0	0.55	2049.91	2643.15	2590.68	2541.04	0.4885	0.3978	0.3865	0.3768
1185.0	0.55	2059.35	2510.9	2458.35	2408.78	0.4635	0.3978	0.3865	0.3768
1205.0	0.55	2077.29	2260.29	2207.56	2158.14	0.4162	0.4012	0.3917	0.3819
1225.0	0.55	2077.29	2260.26	2207.53	2158.11	0.4162	0.4012	0.3917	0.3819
1245.0	0.55	2059.37	2510.65	2458.1	2408.52	0.4635	0.3978	0.3883	0.3786
1265.0	0.55	2059.76	2505.18	2452.62	2403.05	0.4624	0.3979	0.3884	0.3786
1285.0	0.55	2060.28	2497.94	2445.38	2395.81	0.4611	0.398	0.3885	0.3787
1305.0	0.55	2060.9	2489.31	2436.74	2387.18	0.4594	0.3981	0.3886	0.3789
1325.0	0.55	2061.59	2479.61	2427.04	2377.48	0.4576	0.3982	0.3887	0.379
1345.0	0.55	2062.34	2469.08	2416.5	2366.95	0.4556	0.3984	0.3888	0.3791
1365.0	0.55	2063.14	2457.91	2405.33	2355.79	0.4535	0.3985	0.389	0.3793
1385.0	0.55	2063.98	2446.27	2393.67	2344.14	0.4513	0.3987	0.3892	0.3794
1405.0	0.55	2064.84	2434.26	2381.65	2332.12	0.449	0.3988	0.3893	0.3796
1425.0	0.55	2065.72	2421.98	2369.37	2319.85	0.			

1445.0	0.55	2066.61	2409.51	2356.89	2307.38	0.4444	0.3992	0.3896	0.3799
1465.0	0.55	2067.51	2396.92	2344.29	2294.79	0.442	0.3993	0.3898	0.3801
1485.0	0.55	2075.12	2290.68	2237.97	2188.53	0.422	0.4008	0.3913	0.3815
1505.0	0.55	2075.37	2287.24	2234.53	2185.09	0.4213	0.4008	0.3913	0.3816
1525.0	0.55	2075.61	2283.89	2231.18	2181.74	0.4207	0.4009	0.3913	0.3816
1545.0	0.55	2075.84	2280.65	2227.93	2178.5	0.4201	0.4009	0.3914	0.3817
1565.0	0.55	2076.07	2277.51	2224.79	2175.36	0.4195	0.401	0.3914	0.3817
1585.0	0.55	2076.29	2274.5	2221.78	2172.35	0.4189	0.401	0.3915	0.3818
1605.0	0.55	2076.5	2271.63	2218.9	2169.48	0.4184	0.401	0.3915	0.3818
1625.0	0.55	2076.69	2268.88	2216.16	2166.73	0.4178	0.4011	0.3916	0.3818
1645.0	0.55	2076.88	2266.29	2213.56	2164.14	0.4174	0.4011	0.3916	0.3819
1665.0	0.55	2083.72	2171.16	2118.35	2068.99	0.3994	0.4024	0.3929	0.3832
1685.0	0.55	2086.98	2125.81	2072.96	2023.64	0.3908	0.403	0.3935	0.3838
1705.0	0.55	2090.47	2077.34	2024.44	1975.16	0.3817	0.4037	0.3941	0.3844
1725.0	0.55	2094.02	2028.12	1975.17	1925.94	0.3724	0.4043	0.3948	0.3851
1745.0	0.55	2097.51	1979.58	1926.58	1877.39	0.3632	0.405	0.3955	0.3858
1765.0	0.55	2100.9	1932.58	1879.53	1830.38	0.3544	0.4056	0.3961	0.3864
1785.0	0.55	2104.15	1887.5	1834.4	1785.29	0.3459	0.4063	0.3967	0.387
1805.0	0.55	2107.26	1844.5	1791.34	1742.28	0.3377	0.4068	0.3973	0.3876
1005.0	0.6	2078.34	2246.15	2193.4	2143.99	0.4136	0.4014	0.3919	0.3821
1025.0	0.6	2078.2	2248.0	2195.26	2145.85	0.4139	0.4014	0.3918	0.3821
1045.0	0.6	2078.12	2249.08	2196.34	2146.93	0.4141	0.4013	0.3918	0.3821
1065.0	0.6	2078.05	2250.05	2197.31	2147.9	0.4143	0.4013	0.3918	0.3821
1085.0	0.6	2078.0	2250.79	2198.05	2148.64	0.4144	0.4013	0.3918	0.3821
1105.0	0.6	2077.96	2251.29	2198.55	2149.14	0.4145	0.4013	0.3918	0.3821
1125.0	0.6	2077.94	2251.53	2198.79	2149.38	0.4146	0.4013	0.3918	0.3821
1145.0	0.6	2077.94	2251.57	2198.83	2149.42	0.4146	0.4013	0.3918	0.3821
1165.0	0.6	2077.95	2251.42	2198.67	2149.26	0.4145	0.4013	0.3918	0.3821
1185.0	0.6	2077.97	2251.12	2198.38	2148.97	0.4145	0.4013	0.3918	0.3821
1205.0	0.6	2078.0	2250.73	2197.99	2148.58	0.4144	0.4013	0.3918	0.3821
1225.0	0.6	2078.04	2250.26	2197.51	2148.1	0.4143	0.4013	0.3918	0.3821
1245.0	0.6	2078.07	2249.75	2197.0	2147.59	0.4142	0.4013	0.3918	0.3821
1265.0	0.6	2078.11	2249.22	2196.48	2147.07	0.4141	0.4013	0.3918	0.3821
1285.0	0.6	2078.15	2248.7	2195.95	2146.55	0.414	0.4014	0.3918	0.3821
1305.0	0.6	2078.19	2248.2	2195.45	2146.04	0.4139	0.4014	0.3918	0.3821
1325.0	0.6	2078.22	2247.72	2194.98	2145.57	0.4139	0.4014	0.3918	0.3821
1345.0	0.6	2078.34	2246.16	2193.42	2144.01	0.4136	0.4014	0.3919	0.3821
1365.0	0.6	2078.34	2246.15	2193.4	2143.99	0.4136	0.4014	0.3919	0.3821
1385.0	0.6	2077.8	2253.48	2200.74	2151.33	0.4149	0.4013	0.3918	0.382
1405.0	0.6	2077.87	2252.53	2199.79	2150.38	0.4148	0.4013	0.3918	0.3821
1425.0	0.6	2077.93	2251.65	2198.91	2149.5	0.4146	0.4013	0.3918	0.3821
1445.0	0.6	2077.99	2250.82	2198.07	2148.66	0.4144	0.4013	0.3918	0.3821
1465.0	0.6	2078.22	2247.74	2195.0	2145.59	0.4139	0.4014	0.3918	0.3821
1485.0	0.6	2078.23	2247.58	2194.83	2145.43	0.4138	0.4014	0.3918	0.3821
1505.0	0.6	2078.24	2247.42	2194.67	2145.27	0.4138	0.4014	0.3918	0.3821
1525.0	0.6	2078.26	2247.28	2194.53	2145.12	0.4138	0.4014	0.3918	0.3821
1545.0	0.6	2078.27	2247.14	2194.4	2144.99	0.4137	0.4014	0.3918	0.3821
1565.0	0.6	2077.57	2256.93	2204.2	2154.78	0.4156	0.4012	0.3917	0.382
1585.0	0.6	2080.04	2222.41	2169.64	2120.25	0.4091	0.4017	0.3922	0.3825
1605.0	0.6	2082.91	2182.5	2129.69	2080.33	0.4015	0.4022	0.3927	0.383
1625.0	0.6	2086.01	2139.39	2086.55	2037.22	0.3934	0.4028	0.3933	0.3836
1645.0	0.6	2089.21	2094.84	2041.96	1992.67	0.385	0.4034	0.3939	0.3842
1665.0	0.6	2092.43	2050.09	1997.16	1947.91	0.3766	0.404	0.3945	0.3848
1685.0	0.6	2095.62	2005.93	1952.96	1903.74	0.3682	0.4046	0.3951	0.3854
1705.0	0.6	2098.72	1962.88	1909.86	1860.68	0.3601	0.4052	0.3957	0.386
1725.0	0.6	2101.72	1921.2	1868.14	1818.99	0.3522	0.4058	0.3963	0.3866
1745.0	0.6	2104.62	1881.06	1827.95	1778.85	0.3447	0.4063	0.3968	0.3871
1765.0	0.6	2107.41	1842.48	1789.33	1740.26	0.3374	0.4069	0.3973	0.3876
1785.0	0.6	2110.08	1805.5	1752.29	1703.27	0.3304	0.4074	0.3978	0.3881
1805.0	0.6	2078.28	2246.95	2194.21	2144.8	0.4137	0.4014	0.3918	0.3821
1005.0	0.65	2078.34	2246.12	2193.38	2143.97	0.4136	0.4014	0.3919	0.3821
1025.0	0.65	2078.34	2246.13	2193.39	2143.98	0.4136	0.4014	0.3919	0.3821
1045.0	0.65	2078.34	2246.14	2193.39	2143.98	0.4136	0.4014	0.3919	0.3821
1065.0	0.65	2078.34	2246.14	2193.39	2143.98	0.4136	0.4014	0.3919	0.3821
1085.0	0.65	2078.34	2246.13	2193.39	2143.98	0.4136	0.4014	0.3919	0.3821
1105.0	0.65	2078.34	2246.13	2193.38	2143.97	0.4136	0.4014	0.3919	0.3821
1125.0	0.65	2078.34	2246.12	2193.38	2143.97	0.4136	0.4014	0.3919	0.3821
1145.0	0.65	2076.92	2265.3	2212.57	2163.15	0.4172	0.4011	0.3916	0.3819
1165.0	0.65	2076.99	2264.31	2211.58	2162.16	0.417	0.4011	0.3916	0.3819
1185.0	0.65	2077.08	2263.22	2210.49	2161.07	0.4168	0.4011	0.3916	0.3819
1205.0	0.65	2077.16	2262.08	2209.35	2159.93	0.4166	0.4012	0.3916	0.3819
1225.0	0.65	2077.25	2260.9	2208.16	2158.75	0.4163	0.4012	0.3917	0.3819
1245.0	0.65	2077.34	2259.7	2206.96	2157.55	0.4161	0.4012	0.3917	0.382
1265.0	0.65	2078.33	2246.22	2193.47	2144.06	0.4136	0.4014	0.3919	0.3821
1285.0	0.65	2078.34	2246.19	2193.45	2144.04	0.4136	0.4014	0.3919	0.3821
1305.0	0.65	2078.34	2246.17	2193.43	2144.02	0.4136	0.4014	0.3919	0.3821
1325.0	0.65	2078.34	2246.16	2193.41	2144.0	0.4136	0.4014	0.3919	0.3821
1345.0	0.65	2078.34	2246.14	2193.39	2143.98	0.4136	0.4014	0.3919	0.3821
1365.0	0.65	2078.34	2246.12	2193.38	2143.97	0.4136	0.4014	0.3919	0.3821
1385.0	0.65	2076.96	2264.81	2212.08	2162.66	0.4171	0.4011	0.3916	0.3819
1405.0	0.65	2077.07	2263.3	2210.57	2161.15	0.4168	0.4011	0.3916	0.3819
1425.0	0.65	2077.18	2261.84	2209.1	2159.69	0.4165	0.4012	0.3916	0.3819
1445.0	0.65	2077.28	2260.44	2207.71	2158.29	0.4163	0.4012	0.3917	0.3819
1465.0	0.65	2071.5	2341.47	2288.79	2239.32	0.4315	0.4001	0.3906	0.3809
1485.0	0.65	2073.41	2314.85	2262.16	2212.7	0.4265	0.4005	0.3909	0.3812
1505.0	0.65	2075.77	2281.91	2229.2	2179.77	0.4203	0.4009	0.3914	0.3817
1525.0	0.65	2078.47	2244.37	2191.62	2142.22	0.4132	0.4014	0.3919	0.3822
1545.0	0.65	2081.38	2203.87	2151.09	2101.71	0.4056	0.402	0.3924	0.3827
1565.0	0.65	2084.4	2161.78	2108.97	2059.62	0.3976	0.4025	0.393	0.3833
1585.0	0.65	2087.47	2119.13	2066.27	2016.95	0.3896	0.4031	0.3936	0.3839
1605.0	0.65	2090.52	2076.63	2023.75	1974.45	0.3816	0.4037	0.3942	0.3844
1625.0	0.65	2093.54	2034.8	1981.86	1932.62	0.3737	0.4043	0.3947	0.385
1645.0	0.65	2096.48	1993.95	1940.97	1891.76	0.366	0.4048	0.3953	0.3856
1665.0	0.65	2099.34	1954.28	1901.25	1852.08	0.3585	0.4053	0.3958	0.3861
1685.0	0.65	2102.11	1915.89	1862.82	1813.68	0.3512	0.4059	0.3963	0.3866
1705.0	0.65	2075.68	2282.14	2229.42	2179.99	0.4203	0.4009	0.3914	0.3816
1725.0	0.65	2078.32	2246.47	2193.72	2144.31	0.4136	0.4014	0.3919	0.3821
1745.0	0.65	2078.3	2246.66	2193.91	2144.51	0.4137	0.4014	0.3919	0.3821
1765.0	0.65	2078.28	2246.9	2194.16	2144.75	0.4137	0.4014	0.3919	0.3821
1785.0	0.65	2078.26	2247.2	2194.45	2145.04	0.4138	0.4014	0.3918	0.3821
1805.0	0.65	2078.23	2247.56	2194.82	2145.41	0.4138	0.4014	0.3918	0.3821